

# Inactivation of *Pseudomonas aeruginosa* biofilms formed under high shear stress on various hydrophilic and hydrophobic surfaces by a continuous flow of ozonated water

Evgenya S. Shelobolina, Diane K. Walker, Albert E. Parker, Dorian V. Lust, Johanna M. Schultz & Grace E. Dickerman

To cite this article: Evgenya S. Shelobolina, Diane K. Walker, Albert E. Parker, Dorian V. Lust, Johanna M. Schultz & Grace E. Dickerman (2018) Inactivation of *Pseudomonas aeruginosa* biofilms formed under high shear stress on various hydrophilic and hydrophobic surfaces by a continuous flow of ozonated water, Biofouling, 34:7, 826-834, DOI: [10.1080/08927014.2018.1506023](https://doi.org/10.1080/08927014.2018.1506023)

To link to this article: <https://doi.org/10.1080/08927014.2018.1506023>



© 2018 NorthStar Medial Radioisotopes LLC.  
 Published by Informa UK Limited, trading as  
 Taylor & Francis Group.



View supplementary material ↗



Published online: 12 Oct 2018.



Submit your article to this journal ↗



Article views: 1573



View related articles ↗



View Crossmark data ↗



Citing articles: 7 View citing articles ↗

## Inactivation of *Pseudomonas aeruginosa* biofilms formed under high shear stress on various hydrophilic and hydrophobic surfaces by a continuous flow of ozonated water

Evgenya S. Shelobolina<sup>a</sup>, Diane K. Walker<sup>b</sup>, Albert E. Parker<sup>b,c</sup>, Dorian V. Lust<sup>a</sup>, Johanna M. Schultz<sup>b</sup> and Grace E. Dickerman<sup>b</sup>

<sup>a</sup>NorthStar Medical Radioisotopes LLC, Madison, WI, USA; <sup>b</sup>Center for Biofilm Engineering, Montana State University, Bozeman, MT, USA; <sup>c</sup>Department of Mathematical Sciences, Montana State University, Bozeman, MT, USA

### ABSTRACT

The inactivation of *Pseudomonas aeruginosa* biofilms grown on glass under high shear stress and exposed to a range of dissolved ozone concentrations (2, 5 and 7 ppm) at 10 and 20 min was investigated. The regression equation,  $\log \text{reduction (biofilm)} = 0.64 + 0.59 \times (C - 2) + 0.33 \times (T - 10)$ , described the dependence of biofilm inactivation on the dissolved ozone concentration (C, ppm) and contact time (T, min). The predicted D-values were 11.1, 5.7 and 2.2 min at 2, 5 and 7 ppm, respectively. Inactivation of biofilms grown on various surfaces was tested at a single dissolved ozone concentration of 5 ppm and a single exposure time of 20 min. Biofilms grown on plastic materials showed inactivation results similar to that of biofilms on glass, while biofilms grown on ceramics were statistically significantly more difficult to inactivate, suggesting the importance of utilizing non-porous materials in industrial and clinical settings.

### ARTICLE HISTORY

Received 5 February 2018  
Accepted 25 July 2018

### KEYWORDS

Inactivation; biofilm;  
*Pseudomonas aeruginosa*;  
shear stress; dissolved  
ozone; continuous flow

## Introduction

Biofilms are surface-associated communities of microorganisms encased in a protective matrix of highly hydrated extracellular polymeric substances (EPS) (Flemming and Wingender 2010; Flemming et al. 2016). Biofilms constitute the prevalent way of life for microorganisms in both natural and man-made environments. They are often found at a solid–liquid interface and exhibit substantially different attributes than planktonic cells (Donlan and Costerton 2002; Stoodley et al. 2002; Costerton 2004; Hall-Stoodley et al. 2004).


Microbial control and, in particular, biofilm control remains a major challenge for many industries, including the food, medical device and pharmaceutical industries (Anicetti et al. 2015). Biofilm formation follows microbial contamination and is a key strategy that microorganisms use to adapt to changing environments. Once biofilms are formed, they are difficult to remove because the EPS is firmly attached to the surface and can block access of antimicrobial agents to individual cells, leaving behind a source for recontamination. On the other hand, if a biofilm is

disrupted by chemical or mechanical action, a number of compounds can be released that cause immune responses and other reactions in humans.

Ozone is a powerful oxidizing agent that has been studied for applications in the food industry (Khadre et al. 2001; Varga and Szigeti 2016) and in dentistry (Hems et al. 2005; Knight et al. 2008; Domb 2014) as a disinfectant. Lower concentrations that are suboptimal for biofilm inactivation (0.1–2 ppm) were examined in these studies. Food industry and dentistry-related research suggests that ozonated water can be used to control biofilms by preventing their formation (Knight et al. 2008), destroying the surrounding matrix, causing lysis of microorganisms within an established biofilm (Dosti et al. 2005; Robbins et al. 2005; Huth et al. 2009), and/or by destroying endotoxins and other compounds released upon microbial lysis (Rezaee et al. 2008).

The aim of this study was to investigate the ability of ozonated water at 2–7 ppm to inactivate biofilm grown on various surfaces under high shear stress conditions. Ozonated water was continuously applied to *Pseudomonas aeruginosa* biofilms grown with high

**CONTACT** Evgenya S. Shelobolina ✉ [eshelobolina@northstarm.com](mailto:eshelobolina@northstarm.com)

 Supplemental material for this paper is available online at <https://doi.org/10.1080/08927014.2018.1506023>

© 2018 NorthStar Medical Radioisotopes LLC. Published by Informa UK Limited, trading as Taylor & Francis Group. This is an Open Access article distributed under the terms of the Creative Commons Attribution-NonCommercial-NoDerivatives License (<http://creativecommons.org/licenses/by-nc-nd/4.0/>), which permits non-commercial re-use, distribution, and reproduction in any medium, provided the original work is properly cited, and is not altered, transformed, or built upon in any way.

shear and continuous flow in the Center for Disease Control (CDC) biofilm reactor according to a modified version of ASTM E2562-12. Buckingham-Meyer et al. (2007) demonstrated that biofilms grown under high shear stress were the most difficult to inactivate, which suggests that such biofilms are the best models when complete biofilm removal in industrial and clinical settings is targeted. A major advantage of the CDC biofilm reactor (Figure 1) is that it holds 24 coupons (also known as discs or carriers) for biofilm growth. The coupon surfaces can be constructed from a variety of materials (Buckingham-Meyer et al. 2007; Williams and Bloebaum 2009; Coenye and Nelis 2010; Hadi et al. 2010; Azeredo et al. 2017). In this study, two hydrophilic (glass and ceramic) and five hydrophobic plastic (chloro trifluoroethylene HALAR 902 (HALAR), polyether ether ketone (PEEK), ultra-high molecular weight polyethylene Tivar (UHMWPE), ethylene tetrafluoroethylene Tefzel (ETFE), and polyvinylidene difluoride (PVDF)) surfaces were tested for biofilm growth using this method. Biofilm inactivation was assessed using the single tube method (ASTM E2871-13) that was modified for treatment application (Figure 2).

## Materials and methods

### Biofilm reactor

The CDC biofilm reactor is a continuously stirred tank reactor that consists of eight polypropylene rods suspended from a ported UHMWPE lid (Figure 1). Each rod holds three removable sampling coupons (24 in total) of a known surface area on which the biofilms form (Donlan et al. 2004; Goeres et al. 2005).

The assembled lid is mounted in a 1l glass vessel with a side-arm discharge port. The rods are oriented with the coupons perpendicular and equidistant to a baffled stir bar (Buckingham-Meyer et al. 2007), which is rotated by a magnetic stir plate to generate uniform shear.

### Coupon materials

Two hydrophilic materials were tested in this study, borosilicate glass (glass) and glass-mica ceramic (Macor). The five hydrophobic materials were medical industry-related plastics: virgin-grade PEEK, HALAR, UHMWPE, ETFE, and PVDF. From each material, coupons were made with a diameter of 12.7 mm and a thickness of 3.81 mm (except HALAR, at 4.5 mm thick). All the coupons were vertically milled to achieve radial ridges along the surface at a height of 3.18  $\mu\text{m}$ .

### Biofilm growth

ASTM Standard Test Method E2562-12 provides instructions for growing *Pseudomonas aeruginosa* ATCC 700888 on polycarbonate coupons. In this study, ASTM E2562-12 was modified to grow *P. aeruginosa* ATCC 15442, a thicker biofilm former, on the coupon materials listed above. *P. aeruginosa* ATCC 15442 was obtained from American Type Culture Collection (ATCC). In summary, for each experiment, representative morphologies were selected from streak plates made on R2A agar from frozen stock maintained at  $-80^{\circ}\text{C}$ . For inoculation, *P. aeruginosa* was grown in 300 mg  $\text{l}^{-1}$  of tryptic soy broth (TSB) at  $36 \pm 2^{\circ}\text{C}$  in an environmental

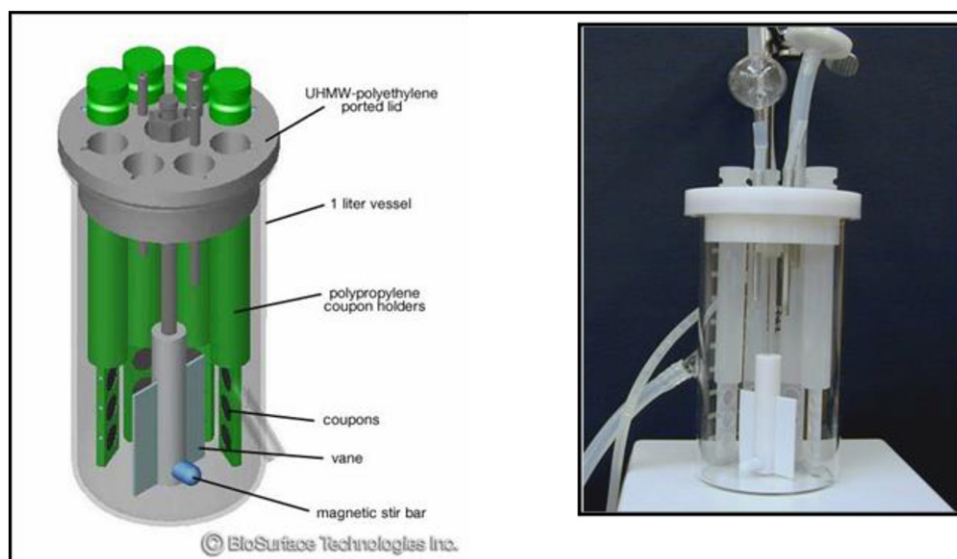


Figure 1. CDC biofilm reactor.

incubator/shaker for 24 h at 110 rpm. One ml of inoculum was injected into a fully assembled, sterile reactor containing 500 ml of 300 mg l<sup>-1</sup> TSB. The reactor was maintained in batch mode (ie baffle stirring and effluent line clamped) for 24 h at room temperature (22 ± 2 °C). After 24 h, the effluent line was unclamped and a continuous flow of 100 mg l<sup>-1</sup> TSB was pumped to the reactor for a residence time of 30 min. After 24 h under continuous flow, the biofilm was ready for treatment application.

### Ozonated water treatment

Ozone was generated electrochemically using an electrolytic cell composed of a diamond coated anode, solid phase electrolyte, and stainless steel cathode sandwiched together (Meas et al. 2011). Two, 5 or 7 ppm ozone concentrations were tested. Reverse osmosis (R/O) water was run through the electrochemical cell and dissolved ozone was maintained at the targeted concentration (± 0.5 ppm) in a mixing beaker by adjusting the current on the cell power supply. The mixing beaker contents were continuously recirculated through the ozone generator. As the contents were pumped out for treatment application, an

equal amount of R/O water was added back to the beaker. A separate loop served to hydrate the cathode (Figure 3).

With the ozonated water stabilized at the targeted concentration, a coupon was removed from the reactor, gently dipped in sterile buffered water to remove any loosely attached or planktonic cells, and transferred to a modified biofilm treatment tube – a conical centrifuge tube (Figure 2A) with holes drilled in it (Figure 2B) to allow for the continuous treatment application of ozonated water to the biofilm-coated coupons. Masterflex silicone tubing size 13 (ID = 0.8 mm) leading from the ozone supply was inserted into the bottom hole of the treatment tube (Figure 2B). Ozonated water (or R/O water alone for controls) was chilled to ~15 °C and pumped to the treatment tube at a flow rate of 89.6 ml min<sup>-1</sup> using a peristaltic pump (Figure 3). The treatment tube was suspended in a 2 l sterile beaker for overflow and placed on a Lab-Line Orbital Shaker set to 120 ± 20 RPM to maximize coupon movement and ensure treatment contact over the entire surface (Figure 3). Ozone measurements were taken every 2 min during the contact time. After treatment application, the coupons were transferred to unmodified conical centrifuge tubes containing neutralizer, 2 × Dey Engley (D/E) neutralizing broth, for harvesting and plating (see Microbial enumeration section for details).

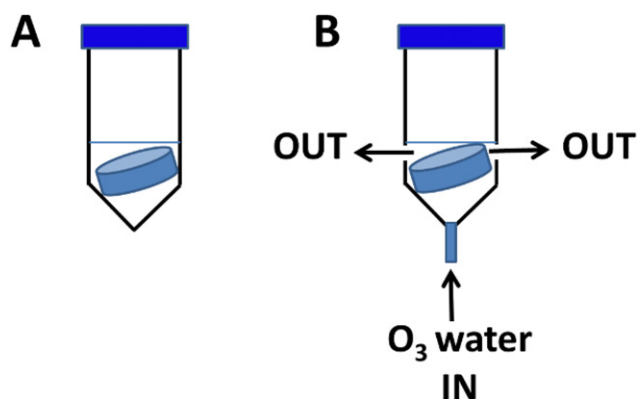


Figure 2. Treatment tube: (A) according to ASTM E2871-13; (B) modified treatment tube used in this study.

### Dissolved ozone measurement

Dissolved ozone concentrations were measured using UV-visible spectrophotometry. The analytical principle of the method is based on the absorption of UV light by the ozone molecule and subsequent use of UV photometry to measure the reduction of light intensity reaching the detector at 254 nm.

The UV absorbance profile of ozone has two regions (Parisse et al. 1996). The absorption spectrum in the 200–310 nm region (Hartley system) consists of

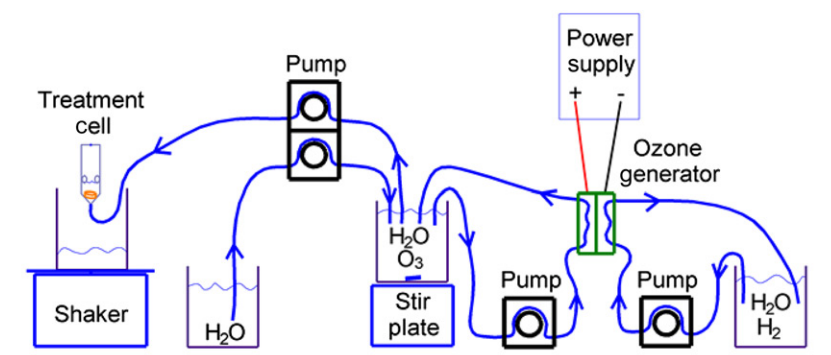


Figure 3. Experimental set-up for ozonated water treatment of *P. aeruginosa* biofilm.

a broad continuum with a maximum at 254 nm. At longer wavelengths (310–350 nm), more intense but diffused bands (Huggins system) predominate. The temperature effect is weak in the Hartley system (Brion et al. 1993), but increases strongly in the Huggins system. Therefore, the Hartley system with a maximum absorbance at 254 nm was used for ozone measurements. At 254 nm, the molar absorption coefficient of ozone is  $2,950 \text{ M}^{-1}\text{cm}^{-1}$  for gas and  $3,300 \text{ M}^{-1}\text{cm}^{-1}$  for ozone dissolved in water (Taube 1956). According to Beer's Law,

$$A_{254} = \alpha C(M) \quad (1)$$

where  $A_{254}$  is absorbance at 254 nm,  $\alpha$  = specific ozone molar absorption coefficient ( $3,300 \text{ M}^{-1}\text{cm}^{-1}$ ), and  $C(M)$  = concentration of ozone (M). Therefore,

$$C(M) = A_{254}/3,300 \quad (2)$$

and the concentration of ozone in ppm is:

$$C(\text{ppm}) = A_{254} \times 48,000/3,300 = A_{254}/0.06875 \quad (3)$$

Dissolved ozone concentrations were measured on a Thermo Scientific Genesys 10S UV-vis spectrophotometer (Waltham, MA, USA).

### Microbial enumeration

The exposed biofilm was neutralized and harvested according to ASTM E2871-13. That is, after the contact time, coupons were transferred to 40 ml  $2 \times$  D/E neutralizing broth and the biofilm was harvested for enumeration. A Scientific Industries Vortex-Genie 2 (Bohemia, NY, USA) set at maximum (10) vortex speed for 30 s was followed by 30 s of sonication using a Transsonic TI-H-15 sonicator at 45 kHz, 10% power, and sweep mode. These steps were repeated with a final 30 s vortexing. Samples were diluted in sterile buffered water ( $0.0425 \text{ g l}^{-1} \text{ KH}_2\text{PO}_4$ ,  $0.405 \text{ g l}^{-1} \text{ MgCl}_2 \cdot 6\text{H}_2\text{O}$ ) and plated on R2A agar using the drop plate method (Herigstad et al. 2001), where 100  $\mu\text{l}$  is distributed between two plates, with five 10  $\mu\text{l}$  drops per plate. Plates were incubated at  $35 \pm 2^\circ\text{C}$  for 24 h. At the end of the incubation period, plates were counted at the dilution containing 3–30 colony forming units (CFU).

### Experimental design

Five experiments were conducted. In the first experiment, biofilms grown on glass coupons were exposed to ozonated water at 2, 5 and 7 ppm dissolved ozone concentrations for 10 min. In the second experiment,

biofilms grown on glass coupons were exposed to ozonated water at 2 and 5 ppm dissolved ozone concentrations for 20 min. For the remaining experiments, biofilms were grown on various hydrophilic and hydrophobic materials and were exposed to ozonated water at 5 ppm dissolved ozone concentration for 20 min. Control coupons were exposed to R/O water for only 10 min during the first experiment and for 20 min during the remaining experiments. Coupons were sampled in triplicate with the exception of two experiments where one of the three replicate control coupons dropped, resulting in only duplicate samples, for a total of 28 controls. A total of 42 coupons were exposed to ozone in this study.

### Statistical analysis

A log reduction (LR) was calculated for each experiment by subtracting the mean  $\log_{10}(\text{CFU cm}^{-2})$  of the coupons treated with ozone from the mean  $\log_{10}(\text{CFU cm}^{-2})$  for the concurrent controls for that same experiment. A linear mixed effects model (lmm) was fit to the  $\log_{10}(\text{CFU cm}^{-2})$  for the untreated control biofilms at 20 min with a random effect for experiment and a fixed effect for surface material (Pinheiro and Bates 2000). A separate lmm was fit to the biofilm LRs at 5 ppm and 20 min that included a fixed effect for surface material with Tukey follow up tests. The LRs for biofilm on glass were analyzed with an lmm with covariates for time and concentration; the corresponding confidence intervals (CI) for the mean LR and prediction intervals (PI) for a LR from a single test were generated using a  $t$  distribution with three degrees of freedom. All statements of statistical significance are with respect to a significance level of 5%. All lmm's were fit using R (R Core Team 2017) package *nlme* (Pinheiro et al. 2017). Model fits, including outlier detection and assessments of the normality and homogeneity of variance assumptions, were assessed via individual value, residual and normal probability plots.

## Results

### Untreated control biofilms

The untreated control data for biofilms grown on the different materials are presented in Tables S1–S3 in the Supplemental material and in Figure 4. The untreated controls contained between  $10^{6.4}$  and  $10^{9.7}$   $\text{CFU cm}^{-2}$  of bacteria depending on the material. The variability of log densities (LD) on the control coupons was analyzed for glass coupons. Glass coupons were used for initial studies and as a control material



for inactivation studies for coupons made of various materials (Tables S1–S3). Forty-three percent of the repeatability variance in the control experiments was due to experiment-to-experiment sources.

The solid line for LDs of control biofilms grown on glass shows the decreasing trend in the LDs between exposures of 10 min and 20 min as was to be expected. The longer the exposure of the control coupons to continuously flowing water, the more likely biofilm cells will be flushed off the coupon surface.

Although the average LD of control biofilms grown on various materials at 20 min of exposure ranged from 6.8 (PEEK) to 9.3 (PVDF) (Table S3), the

differences among materials were not statistically significant ( $p \geq 0.056$ ).

#### *Dissolved ozone efficacy against biofilms grown on glass*

In four of the experiments, the biofilms were grown on glass to investigate biofilm inactivation at three different ozone concentrations ( $C = 2, 5$  and  $7$  ppm) and two contact times ( $T = 10$  and  $20$  min) (Figure 5 and Tables S1–S3).

The regression equation that describes the LR of biofilm caused by dissolved ozone exposure is:

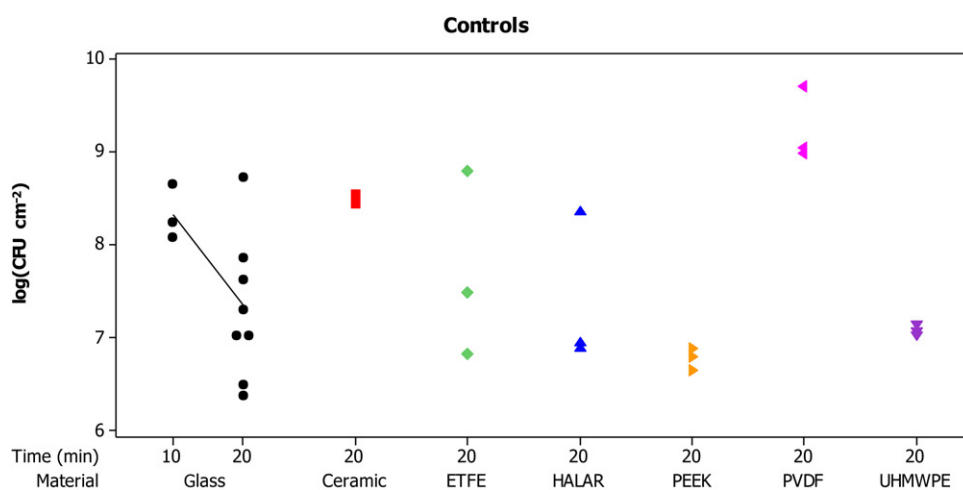


**Figure 4.** Biofilm abundances recovered from the untreated control coupons over three experiments. The solid line for biofilms grown on glass shows the decreasing trend between the 10 min and 20 min contact times. The results for each material were generated by a separate independent experiment except for glass at 20 min, where the results were collected over four experiments. Each point in the figure is the  $\log(\text{CFU cm}^{-2})$  for a single coupon in a single experiment.

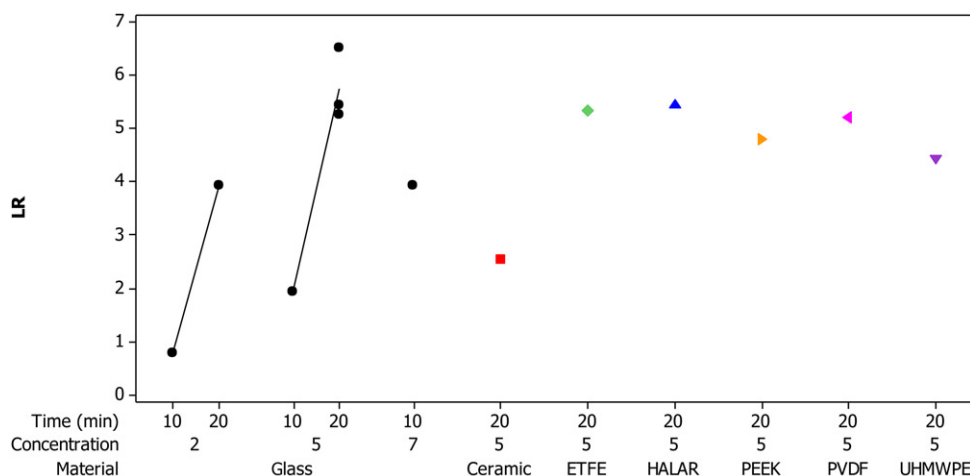


**Figure 5.** The log reductions of biofilms grown on different materials for different ozone concentrations and contact times. The solid line for biofilms grown on glass shows the increasing trend between the 10 min and 20 min contact times at 2 ppm and 5 ppm. Biofilms on glass were studied in four experiments. Each of the other materials were studied only in a single experiment for a total of three experiments. Each point in the figure is the LR attained for a single concentration and contact time of ozone in a single experiment.

$$LR_{\text{biofilm}} = 0.64 + 0.59 \times (C - 2) + 0.33 \times (T - 10) \quad (4)$$

where  $C$  is dissolved ozone concentration (ppm) and  $T$  is contact time (min). This regression equation allows calculation of a  $D$ -value, the time required to inactivate 90% of cells (one LR). The  $D$ -values are 11.1, 5.7 and 2.2 min at 2, 5 and 7 ppm, respectively.

Figure 6 offers a visualization of this equation for the concentrations tested, overlaid on the LR data from the four experiments where biofilms were grown

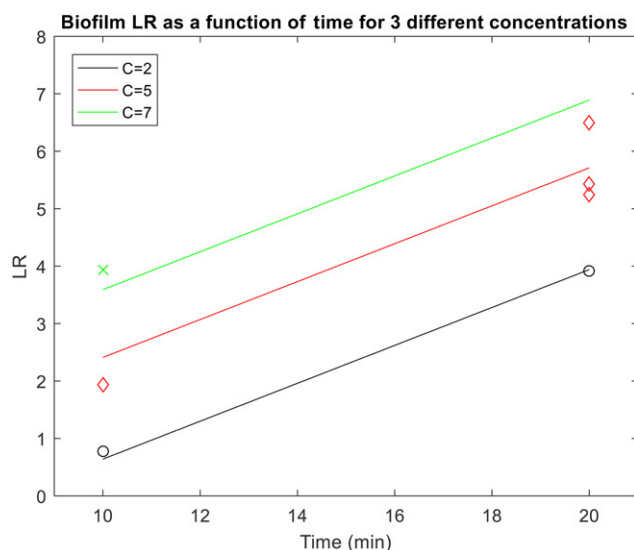


**Figure 6.** Predicted log reduction of biofilms on glass. The regression equation is visualized as a solid line for 2, 5 and 7 ppm, the actual concentrations tested. Each point in the figure is the log reduction attained for a particular concentration and contact time of ozone in a single experiment.

on glass. The repeatability SD of the LRs for treated biofilms was 0.61 logs with 38% of the variability due to experiment-to-experiment sources. This is an acceptable repeatability as compared to other LRs for *in vitro* tests of antimicrobials (Tilt and Hamilton 1999). Figure 7 offers two summaries of the minimal LR, at 95% confidence, attained for any combination of ozone concentration and contact time based on the regression equation. Figure 7A shows the minimum mean LR over many experiments and Figure 7B shows the minimum LR for a single experiment, at 95% confidence.

### Dissolved ozone efficacy against biofilms grown on different materials

Inactivation of *P. aeruginosa* biofilms grown on ceramics and five plastic surfaces was also studied (Table S3 and Figure 4). At 5 ppm and 20 min, biofilms grown on ceramics were statistically significantly harder to inactivate (with a LR = 2.6 attained in a single experiment) compared to any other materials ( $p \leq 0.048$ ) except PVDF ( $p = 0.156$ ). Table 1 shows a comparison of LR for ceramics vs other materials. Even though the LR for ceramics was estimated to be 2.07 more than the LR for PVDF, this difference was not statistically significant ( $p = 0.156$ ). One reason for the lack of significance was due to an increased variability owing to the experiments for inactivation of biofilms grown on ceramics and PVDF were carried out on different days (ie the difference fell within the experiment-to-experiment variability).

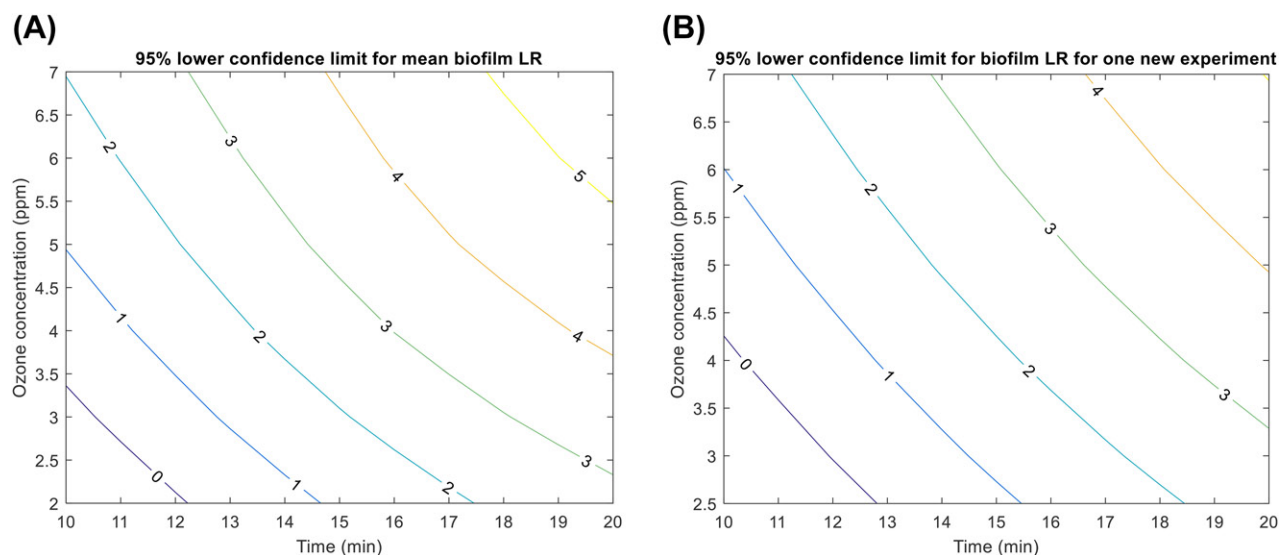


**Figure 7.** Predicted minimum log reduction at 95% confidence due to different concentrations and contact times of an ozone treatment. (A) Minimum mean log reduction over many experiments; (B) minimum log reduction for a single experiment.

**Table 1.** Comparison of log reduction (LR) for ceramics vs other materials.

Materials compared	Difference between LR	Standard error (SE)	p-value
Glass, ceramics	3.18	0.773	<0.001
ETFE, ceramics	2.78	0.464	<0.001
HALAR, ceramics	3.10	0.851	0.004
PEEK, ceramics	2.46	0.851	0.048
PVDF, ceramics	2.07	0.851	0.156
UHMWPE, ceramics	1.88	0.464	<0.001

No bacteria were detected on 22 of the 42 coupons after exposure to ozone. In these cases, a value of 0.5 CFU was substituted for the total volume enumerated at the lowest dilution to enable calculation of a  $\log_{10}$ -transformed CFU  $\text{cm}^{-2}$  value. This sets the effective limit of detection for the method at 48.4 CFU  $\text{cm}^{-2}$  for all coupon materials except HALAR. HALAR coupons had a slightly larger surface area (4.32  $\text{cm}^2$ ), which sets the effective limit of detection for HALAR coupons at 46.3 CFU  $\text{cm}^{-2}$ . Hence, the LRs reported here, and the efficacy of ozone, are underestimated in this study (Singh and Nocerino 2002).

## Discussion

The aim of this study was to investigate the ability of continuously applied ozonated water at high concentrations (2–7 ppm) to inactivate biofilms grown on various surfaces under high shear stress. Previous studies on biofilm inactivation by continuously applied ozonated water were carried out either at lower dissolved ozone concentrations (0.6–0.7 ppm dissolved ozone) (Dosti et al. 2005; Hems et al. 2005) or with biofilms grown without shear stress (Robbins et al. 2005). In this study, *P. aeruginosa* biofilms were grown under high shear stress using ASTM E2562-12 and inactivated using ASTM E2871-13. Biofilms grown under high shear stress are better models for complete biofilm removal in studies relevant to industrial and clinical settings as they are more difficult to inactivate (Buckingham-Meyer et al. 2007). The treatment tube in ASTM E2871-13 was modified to allow continuous flow of ozonated water.

Inactivation experiments with *P. aeruginosa* biofilm grown on glass allowed the derivation of a regression equation describing the dependency of the LR on dissolved ozone concentration.

In addition, effect of ozonated water was tested against *P. aeruginosa* biofilms grown on various hydrophilic (glass and ceramics) and hydrophobic (HALAR, PEEK, UHMWPE, ETFE, and PVDF) plastic surfaces. Several surface properties of the materials influence biofilm formation and/or removal

(Darouiche 2001), including surface wettability (Darouiche 2001; Gomez-Suarez et al. 2001). Based on the results of the current study, surface wettability did not seem to affect biofilm removal. All the hydrophobic materials, including HALAR, PEEK, UHMWPE, ETFE, and PVDF showed results similar to glass. This could be attributed to a conditioning film being formed during the first stage of the biofilm development which modified the properties of the original surface (Daeschel and McGuire 1998; Hori and Matsumoto 2010; Simoes et al. 2010).

Another important property is the topography of the surface. A great body of the research has been carried out into the links between surface topography and microbial retention in biomedical applications (Guo et al. 2017; Skoog et al. 2018), food science (Masurovsky and Jordan 1958; Verran et al. 2001; Verran et al. 2010), microbial fuel cells (Santoro et al. 2014), material science (Pedersen 1990), and geological microbiology (Miller et al. 2012). A general observation from these various applications is that microorganisms attached in greater numbers to and were better retained on irregular and textured than regular and smooth surfaces.

In this study all the coupons were machined so that they had a similar surface finish with an average roughness of 125  $\mu\text{m}$  (3.18  $\mu\text{m}$ ). However, the biofilms grown on ceramics were statistically significantly more difficult to inactivate than the biofilms grown on glass ( $p < 0.001$ ). Similar results were obtained for *Acinetobacter baumannii* biofilms (Ivankovic et al. 2017): biofilms grown on ceramics were more resistant to inactivation by benzalkonium chloride and chlorhexidine than the biofilms grown on glass. One possible explanation for these results is that unlike glass and the tested plastic materials, ceramic materials can have different degrees of porosity. Multiple studies have emphasized the importance of nano- and micro-scale surface features for microbial retention (Whitehead et al. 2006; Anselme et al. 2010; Verran et al. 2010; Crawford et al. 2012; Nikkhah et al. 2012; Hsu et al. 2013; Santoro et al. 2014; Skoog et al. 2018; Vazquez-Nion et al. 2018), including an open porosity correlating with the growth of a phototrophic biofilm on the surfaces of granitic rocks (Vazquez-Nion et al. 2018), scratches and pits on food preparation surfaces providing niches in which protect microorganisms from shear forces and cleaning (Verran et al. 2010), and the quantity of biofilm attached to electrodes in microbial fuel cell being positively correlated to the number of small scale (5–10  $\mu\text{m}$ ) pores on the electrode surface (Santoro et al. 2014). This collection of



results suggests that extra care should be taken to ensure materials with low to zero porosity are utilized in industrial and clinical settings.

As previously stated by Crawford et al. (2012), a description of micrometer and sub-micrometer levels of roughness is essential when investigating the interactions between bacterial cells and the material surface and the minimum set of parameters for such investigations should include description of both, vertical and horizontal dimensions of the surface. In conclusion more in-depth experiments are required to correlate porosity and other surface features of ceramics with biofilm inactivation.

## Disclosure statement

No potential conflict of interest was reported by the authors.

## References

- Anicetti V, Mittelman M, Adley C, Amin P, Arigo J, Baseman H, Bevel JP, Clontz L, Deutschmann S, Devine RA et al. 2015. Bioburden and biofilm management in pharmaceutical manufacturing operations: Technical report no. 69. Bethesda (MD): Parenteral Drug Association, Inc; p. 1–67.
- Anselme K, Davidson P, Popa AM, Giazon M, Liley M, Ploux L. 2010. The interaction of cells and bacteria with surfaces structured at the nanometre scale. *Acta Biomater.* 6:3824–3846. doi:10.1016/j.actbio.2010.04.001
- Azeredo J, Azevedo NF, Briandet R, Cerca N, Coenye T, Costa AR, Desvaux M, Di Bonaventura G, Hebraud M, Jaglic Z, et al. 2017. Critical review on biofilm methods. *Crit Rev Microbiol.* 43:313–351. doi:10.1080/1040841X.2016.1208146
- Brion J, Chakir A, Daumont D, Malicet J, Parisse C. 1993. High-resolution laboratory absorption cross-section of O<sub>3</sub> - temperature effect. *Chem Phys Lett.* 213:610–612. doi:10.1016/0009-2614(93)89169-I
- Buckingham-Meyer K, Goeres D, Hamilton MA. 2007. Comparative evaluation of biofilm disinfectant efficacy tests. *J Microbiol Methods.* 70:236–244. doi:10.1016/j.mimet.2007.04.010
- Coenye T, Nelis HJ. 2010. In vitro and in vivo model systems to study microbial biofilm formation. *J Microbiol Methods.* 83:89–105. doi:10.1016/j.mimet.2010.08.018
- Costerton JW. 2004. A short history of the development of the biofilm concept. In: Ghannoum MA, O'Toole G, editors. *Microbial Biofilms*. Washington, DC: ASM Press; p. 4–19.
- Crawford RJ, Webb HK, Truong VK, Hasan J, Ivanova EP. 2012. Surface topographical factors influencing bacterial attachment. *Adv Colloid Interface Sci.* 179:142–149.
- Daeschel MA, McGuire J. 1998. Interrelationships between protein surface adsorption and bacterial adhesion. *Biotechnol Bioeng Rev.* 15:413–438. doi:10.1080/02648725.1998.10647964
- Darouiche RO. 2001. Device-associated infections: a macro-problem that starts with microadherence. *Clin Infect Dis.* 33:1567–1572. doi:10.1086/323130
- Domb WC. 2014. Ozone therapy in dentistry. A brief review for physicians. *Interv Neuroradiol.* 20:632–636. doi:10.15274/INR-2014-10083
- Donlan RM, Costerton JW. 2002. Biofilms: Survival mechanisms of clinically relevant microorganisms. *Clin Microbiol Rev.* 15:167. doi:10.1128/CMR.15.2.167-193.2002
- Donlan RM, Priede JA, Heyes CD, Sanii L, Murga R, Edmonds P, El-Sayed I, El-Sayed MA. 2004. Model system for growing and quantifying *Streptococcus pneumoniae* biofilms in situ and in real time. *Appl Environ Microbiol.* 70:4980–4988. doi:10.1128/AEM.70.8.4980-4988.2004
- Dosti B, Guzel-Seydim Z, Greene AK. 2005. Effectiveness of ozone, heat and chloride for destroying common food spoilage bacteria in synthetic media and biofilms. *Int J Dairy Technol.* 58:19–24. doi:10.1111/j.1471-0307.2005.00176.x
- Flemming HC, Wingender J. 2010. The biofilm matrix. *Nat Rev Microbiol.* 8:623–633. doi:10.1038/nrmicro2415
- Flemming HC, Wingender J, Szewzyk U, Steinberg P, Rice SA, Kjelleberg S. 2016. Biofilms: an emergent form of bacterial life [Review]. *Nat Rev Microbiol.* 14:563–575. doi:10.1038/nrmicro.2016.94
- Goeres D, Loetterie LR, Hamilton MA, Murga R, Kirby DW, Donlan RM. 2005. Statistical assessment of a laboratory method for growing biofilms. *Microbiology.* 151:757–762. doi:10.1099/mic.0.27709-0
- Gomez-Suarez C, Busscher HJ, Van Der Mei HC. 2001. Analysis of bacterial detachment from substratum surfaces by the passage of air-liquid interfaces. *Appl Environ Microbiol.* 67:2531–2537. doi:10.1128/AEM.67.6.2531-2537.2001
- Guo SS, Zhu XY, Loh XJ. 2017. Controlling cell adhesion using layer-by-layer approaches for biomedical applications. *Mater Sci Eng C Mater Biol Appl.* 70:1163–1175. doi:10.1016/j.msec.2016.03.074
- Hadi R, Vickery K, Deva A, Charlton T. 2010. Biofilm removal by medical device cleaners: comparison of two bioreactor detection assays. *J Hosp Infect.* 74:160–167. doi:10.1016/j.jhin.2009.10.023
- Hall-Stoodley L, Costerton JW, Stoodley P. 2004. Bacterial biofilms: from the natural environment to infectious diseases. *Nat Rev Microbiol.* 2:95–108. doi:10.1038/nrmicro821
- Hems RS, Gulabivala K, Ng Y-L, Ready D, Spratt DA. 2005. An in vitro evaluation of the ability of ozone to kill a strain of *Enterococcus faecalis*. *Int Endod J.* 38:22–29. doi:10.1111/j.1365-2591.2004.00891.x
- Herigstad B, Hamilton M, Heersink J. 2001. How to optimize the drop plate method for enumerating bacteria. *J Microbiol Methods.* 44:121–129. doi:10.1016/S0167-7012(00)00241-4
- Hori K, Matsumoto S. 2010. Bacterial adhesion: From mechanism to control. *Biochem Eng J.* 48:424–434. doi:10.1016/j.bej.2009.11.014
- Hsu LC, Fang J, Borca-Tasciuc DA, Worobo RW, Moraru CI. 2013. Effect of micro- and nanoscale topography on the adhesion of bacterial cells to solid surfaces. *Appl Environ Microbiol.* 79:2703–2712. doi:10.1128/AEM.03436-12
- Huth KC, Quirling M, Maier S, Kamereck K, AlKhayer M, Paschos E, Welsch U, Miethke T, Brand K, Hickel R. 2009. Effectiveness of ozone against endodontopathogenic microorganisms in a root canal biofilm model. *Int Endod J.* 42:3–13. doi:10.1111/j.1365-2591.2008.01460.x
- Ivankovic T, Goic-Barisic I, Hrenovic J. 2017. Reduced susceptibility to disinfectants of *Acinetobacter baumannii*

- biofilms on glass and ceramic. *Arh Hig Rada Toksikol.* 68:99–108. doi:10.1515/aiht-2017-68-2869
- Khadre MA, Yousef AE, Kim JG. 2001. Microbiological aspects of ozone applications in food: a review. *J Food Sci.* 66:1242–1252. doi:10.1111/j.1365-2621.2001.tb15196.x
- Knight GM, McIntyre JM, Craig GG, Mulyani, Zilm PS. 2008. The inability of *Streptococcus mutans* and *Lactobacillus acidophilus* to form a biofilm in vitro on dentine pretreated with ozone. *Aust Dent J.* 53:349–353. doi:10.1111/j.1834-7819.2008.00077.x
- Masurovsky EB, Jordan WK. 1958. Studies on the relative bacterial cleanability of milk-contact surfaces. *J Dairy Sci.* 41:1342–1358. doi:10.3168/jds.S0022-0302(58)91098-1
- Meas Y, Godinez LA, Bustos E. 2011. Ozone generation using boron-doped diamond electrodes. In: Brillas E, Martinez-Huitle CA, editors. *Synthetic diamond films: preparation, electrochemistry, characterization, and application.* Hoboken (NJ): John Wiley & Sons; p. 311–331.
- Miller AZ, Sanmartin P, Pereira-Pardo L, Dionisio A, Saiz-Jimenez C, Macedo MF, Prieto B. 2012. Bioreceptivity of building stones: a review. *Sci Total Environ.* 426:1–12. doi:10.1016/j.scitotenv.2012.03.026
- Nikkhah M, Edalat F, Manoucheri S, Khademhosseini A. 2012. Engineering microscale topographies to control the cell-substrate interface. *Biomater.* 33:5230–5246. doi:10.1016/j.biomaterials.2012.03.079
- Parisse C, Brion J, Malicet J. 1996. UV absorption spectrum of ozone: structure analysis and study of the isotope effect in the Harley system. *Chem Phys Lett.* 248:31–36. doi:10.1016/0009-2614(95)01259-1
- Pedersen K. 1990. Biofilm development on stainless steel and PVC surfaces in drinking water. *Water Res.* 24:239–243. doi:10.1016/0043-1354(90)90109-J
- Pinheiro J, Bates D. 2000. Mixed effects models in S and S-PLUS. New York: Springer-Verlag.
- Pinheiro J, Bates D, DebRoy S, Sarkar D, Team RC. 2017. Package nlme: linear and nonlinear mixed effects models. R package version 31-131.
- R Core Team. 2017. R: A language and environment for statistical computing. Vienna, Austria: R Foundation for Statistical Computing. <http://www.R-project.org/>
- Rezaee A, Ghanizadeh G, Yazdanbakhsh AR, Behzadiannejad G, Ghaneian MT, Siyadat SD, Hajizadeh E. 2008. Removal of endotoxin in water using ozonation process. *Aust J Basic Appl Sci.* 2:495–499.
- Robbins JB, Fisher CW, Moltz AG, Martin SE. 2005. Elimination of *Listeria monocytogenes* biofilms by ozone, chlorine, and hydrogen peroxide. *J Food Prot.* 68:494–498. doi:10.4315/0362-028X-68.3.494
- Santoro C, Guilizzoni M, Baena JPC, Pasaogullari U, Casalegno A, Li B, Babanova S, Artyushkova K, Atanassov P. 2014. The effects of carbon electrode surface properties on bacteria attachment and start up time of microbial fuel cells. *Carbon.* 67:128–139. doi:10.1016/j.carbon.2013.09.071
- Simoes M, Simoes LC, Vieira MJ. 2010. A review of current and emergent biofilm control strategies. *LWT Food Sci Technol.* 43:573–583. doi:10.1016/j.lwt.2009.12.008
- Singh A, Nocerino J. 2002. Robust estimation of mean and variance using environmental data sets with below detection limit observations. *Chemometr Intell Lab Syst.* 60:69–86. doi:10.1016/S0169-7439(01)00186-1
- Skoog SA, Kumar G, Narayan RJ, Goering PL. 2018. Biological responses to immobilized microscale and nanoscale surface topographies. *Pharmacol Ther.* 182:33–55. doi:10.1016/j.pharmthera.2017.07.009
- Stoodley P, Sauer K, Davies DG, Costerton JW. 2002. Biofilms as complex differentiated communities. *Annu Rev Microbiol.* 56:187–209. doi:10.1146/annurev.micro.56.012302.160705
- Taube H. 1956. Photochemical reactions of ozone in solution. *Phys Chem Chem Phys.* 53:656–665.
- Tilt N, Hamilton MA. 1999. Repeatability and reproducibility of germicide tests: a literature review. *J AOAC Int.* 82:384–389.
- Varga L, Szigeti J. 2016. Use of ozone in the dairy industry: a review. *Int J Dairy Technol.* 69:157–168.
- Vazquez-Nion D, Silva B, Prieto B. 2018. Influence of the properties of granitic rocks on their bioreceptivity to sub-aerial phototrophic biofilms. *Sci Total Environ.* 610:44–54.
- Verran J, Packer A, Kelly PJ, Whitehead KA. 2010. Use of the atomic force microscope to determine the strength of bacterial attachment to grooved surface features. *J Adhes Sci Technol.* 24:2271–2285.
- Verran J, Rowe DL, Boyd RD. 2001. The effect of nanometer dimension topographical features on the hygienic status of stainless steel. *J Food Prot.* 64:1183–1187.
- Whitehead KA, Rogers D, Colligon J, Wright C, Verran J. 2006. Use of the atomic force microscope to determine the effect of substratum surface topography on the ease of bacterial removal. *Colloids Surf B Biointerfaces.* 51:44–53.
- Williams DL, Bloebaum RD. 2009. Observing the biofilm matrix of *Staphylococcus epidermidis* ATCC 35984 grown using the CDC biofilm reactor. *Microsc Microanal.* 15:824–825.